Electronic structure and electric-field gradients for $YBa_2Cu_4O_8$ from density-functional calculations

Claudia Ambrosch-Draxl,* Peter Blaha, and Karlheinz Schwarz
Institut für Technische Elektrochemie, Technische Universität Wien, A-1060 Vienna, Getreidemarkt 9/158, Austria
(Received 22 April 1991)

The band structure, densities of states, partial charges, electron densities, and electric-field gradients (EFG's) of $YBa_2Cu_4O_8$ are determined from first-principles calculations using the full-potential linearized-augmented-plane-wave method. Exchange and correlation effects are treated by the local-density approximation. The doubling of the copper-oxygen chains with respect to $YBa_2Cu_3O_7$ affects the electronic structure, especially near the chain oxygen, which has a third copper neighbor. The charge distribution around this position is drastically changed, and consequently the asymmetry parameter of the EFG is increased from 0.3 to 1.0, while the principal EFG component becomes similar for all oxygen positions. The bonding characteristic of the double chains is illustrated by difference electron densities. The core-level shifts are estimated and agree with experimental data, which are available for Ba and Y.

I. INTRODUCTION

$YBa_2Cu_3O_7$ (Y-Ba-Cu-O_7) is the well-known 90-K superconductor in the class of ceramic high-T_c materials. When the oxygen content in Cu-O chains is reduced, superconductivity is lost, yielding the antiferromagnetic insulator $YBa_2Cu_3O_6$ (Y-Ba-Cu-O_6). Karpinski *et al.*[1] have synthesized samples where the Cu-O chains are doubled along the c axis with an in-plane displacement parallel to the b axis (Fig. 1). In this new 80-K superconductor $YBa_2Cu_4O_8$ (Y-Ba-Cu-O_8) with the orthorhombic space group *Ammm*, the c axis is about doubled. The double chain causes a much higher stability at higher temperatures in terms of oxygen content. It has been found by Kaldis *et al.*[2] that the critical temperature rises significantly under hydrostatic pressure, namely, by 0.55 K/kbar, and that the bridging oxygen O(4) moves toward the Cu-O plane, implying a charge transfer to the latter. A similar change in position of the apical oxygen has already been observed when Y-Ba-Cu-O_6 is oxidized to Y-Ba-Cu-O_7,[3] but in this case the total electron-hole concentration is increased as well.

The electric-field gradient (EFG) is a ground-state property of a solid depending sensitively on the asymmetry of the electronic charge around a nucleus and thus gives detailed information about the charge distribution in a crystal. Experimentally, the EFG in Y-Ba-Cu-O_8 has been measured at the copper sites by nuclear magnetic resonance (NMR) and nuclear quadrupole resonance (NQR) spectroscopy.[4,5]

In 1985 Blaha, Schwarz, and Herzig[6] developed a first-principles method to compute EFG's from a full-potential linearized-augmented-plane-wave (LAPW) band-structure calculation. They have calculated the EFG directly from the self-consistent charge density by solving Poisson's equation without further approximations. Since this method was successfully applied to various systems, such as Li_3N,[6] hcp metals,[7] or Cu_2O,[8] the study of the complicated high-T_c materials is well founded. We have already performed such calculations for Y-Ba-Cu-O_7, Y-Ba-Cu-$O_{6.5}$, and Y-Ba-Cu-O_6 and found good agreement with experimental EFG's except for the

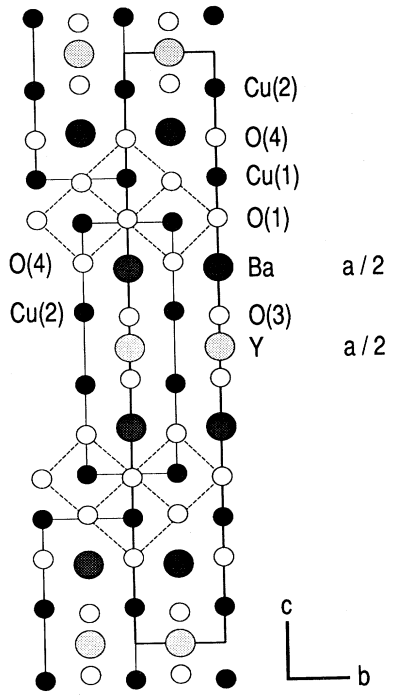

FIG. 1. Projection of the Y-Ba-Cu-O_8 crystal structure onto the b-c plane. The fine lines indicate the Y-Ba-Cu-O_7 building blocks, and the bold lines characterize the Y-Ba-Cu-O_8 unit cell. The Cu(1)-O(1) chains are doubled along the c axis with a displacement of half a lattice parameter b, so that the Cu(1) atoms have four O(1) neighbors (dashed lines) and the chains become buckled. The c parameter of Y-Ba-Cu-O_8 is more than twice that of Y-Ba-Cu-O_7.

Cu(2) position in the CuO_2 plane.[9-11]

We present a detailed analysis of the electronic structure and EFG of these systems, providing information on the role of Cu-O planes and chains especially in terms of charge distribution. This gives a basis for investigating the electron dynamics on a small energy scale appropriate for a fundamental understanding of superconductivity. During the preparation of the manuscript, two band-structure calculations for Y-Ba-Cu-O_8 appeared in literature.[12,13]

II. COMPUTATIONAL DETAILS

We have performed full-potential LAPW calculations using the WIEN code.[14] Atomic sphere radii of 2.74, 2.9, 1.9, and 1.55 a.u. are taken for Y, Ba, Cu, and O, respectively. Up to 1340 basis functions are used, and the expansion of the radial wave function is limited to $l=12$. Inside the atomic spheres the potential and charge density are expanded in crystal harmonics up to $L=4$; in the interstitial region a Fourier series with 1554 stars of K is used. Since the charges of Y 4s, Y 4p, Ba 5s, and Cu 3p states are not completely confined inside the respective atomic spheres, these states are treated as semicore in an additional band calculation. For the Brillouin-zone (BZ) integrations, 64 (8) k points are used for the valence (semicore) states, representing 343 (27) k points in the whole BZ. The structural parameters are taken from Kaldis *et al.*[2] using data at 145 K.

III. ELECTRIC-FIELD GRADIENT

All nuclei with a nuclear-spin quantum number $I \geq 1$ have a nonspherical nuclear charge distribution and an electric quadrupole moment Q. The nuclear quadrupole interaction between this Q and the electric-field gradient (EFG) determines the NQ coupling constant eQV_{zz}/h, where e is the electric charge, h is Planck's constant, and V_{zz} represents the principal component of the EFG. The EFG is defined as the second derivative of the electrostatic potential at the nuclear position written as traceless tensor.

Blaha, Schwarz, and Herzig were the first to compute the EFG by a first-principles method.[6] This scheme is based on a full-potential LAPW calculation in which the unit cell is divided into nonoverlapping atomic spheres and in an interstitial region; the potential (and, analogously, the charge density) is written as radial function $v_{LM}(r)$ times symmetrized spherical harmonics $Y_{LM}(\hat{\mathbf{r}})$ inside the spheres and as Fourier series in the interstitial region. For a given charge density, the Coulomb potential is obtained numerically by solving Poisson's equation in form of a boundary-value problem using a method proposed by Weinert.[15] This yields the potential coefficients $v_{LM}(r)$, which, in the limit $r \to 0$, has the asymptotic form $v_{LM}(r)=r^L V_{LM}$. For the EFG calculation only the $L=2$ terms near the nucleus contribute. A more detailed description of the formalism is given in Ref. 11. With these definitions the diagonal terms of the traceless EFG tensor with respect to the crystallographic axes a, b, and c are

$$V_{aa} = -\tfrac{1}{2}V_{20} + V_{22} ,$$
$$V_{bb} = -\tfrac{1}{2}V_{20} - V_{22} , \quad (1)$$
$$V_{cc} = V_{20} .$$

In Y-Ba-Cu-O_8 the off-diagonal elements of the EFG tensor at all sites vanish due to symmetry, so that the principal axis of the EFG coincides with one of the crystallographic axes. By ordering the components according to their magnitudes, we define

$$|V_{zz}| \geq |V_{yy}| \geq |V_{xx}| . \quad (2)$$

The EFG tensor is characterized by the largest component V_{zz} (in short, EFG) and the anisotropy parameter η defined as

$$\eta = (V_{xx} - V_{yy})/V_{zz} , \quad (3)$$

where η varies between 0 (axial symmetry) and 1 ($V_{xx}=0$).

IV. RESULTS

A. Band structure and densities of states

The Brillouin zone (BZ) corresponding to the actual crystal dimensions of Y-Ba-Cu-O_8 is displayed in Fig. 2. The energy bands are shown in Fig. 3 where one notes that the bands are very similar along the Λ and H symmetry directions (Fig. 1), which are parallel lines at the center and top of the BZ. This observation illustrates that the dispersion in the k_z direction is small. The most noticeable difference occurs for the two bands just below E_F, which show a smaller splitting at Z than at T. The Fermi energy falls in the antibonding region of the Cu(1)-O(1)-O(4) and Cu(2)-O(2)-O(3) bands as in Y-Ba-Cu-O_7 and is discussed below. The total density of states (DOS) at E_F (of 3.8 states per eV and formula unit) is smaller than that of Y-Ba-Cu-O_7 in parallel with the

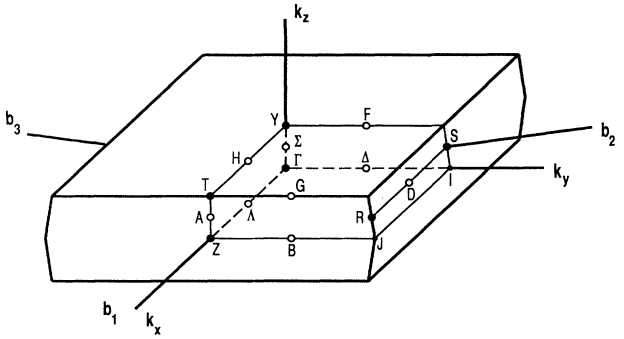

FIG. 2. First Brillouin zone for the orthorhombic lattice with space group *Ammm* using the actual cell dimension: the solid circles denote symmetry points, the open circles symmetry lines. The k points I and J are no high-symmetry points, but are labeled for clarity.

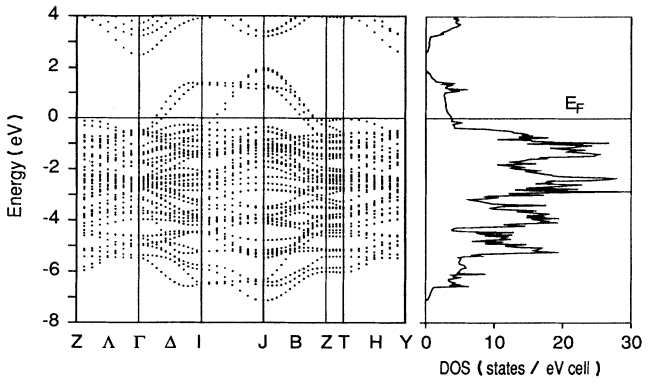

FIG. 3. Band structure and total density of states of Y-Ba-Cu-O_8. The DOS is given in states (including spin) per eV and formula unit.

lower T_c, although the relation between the DOS and T_c seems to be different than with conventional superconductors.

The band structure of Y-Ba-Cu-O_8 is quite similar to that of Y-Ba-Cu-O_7,[16–18] but in Y-Ba-Cu-O_8 (Y-Ba-Cu-O_7) four (three) bands cross the Fermi energy along the B direction (between S and X), where the additional band originates from the second Cu(1)-O(1) chain. This can be seen from Fig. 4, which allows us to see how much the various copper and oxygen positions contribute to each band state. For that purpose a section of the band structure (along the B direction) is repeated and each band state is characterized by its site-dependent charge contribution. (The size of each circle is proportional to the partial charge of the specified atom.) The section for O(2) is omitted in Fig. 4, since it is essentially the same as that for O(3). Four antibonding bands cross E_F where the higher two have predominantly Cu(2), O(2), and O(3) character and correspond to pd_σ bonds, while the other two show strong Cu(1)-O(1) and some Cu(1)-O(4) interactions and originate from the double chains. Near 0.4 Ry flat nonbonding bands of Cu(1) or Cu(2) character with little admixture from oxygen states occur and at even lower energies various states can be seen which show strong dispersion and come from Cu-O bonding interactions.

The site-projected densities of states (Fig. 5) demonstrate again the strong covalent character of the Cu(1)-O(1)-O(4) and the Cu(2)-O(2)-O(3) bands [the O(2) contribution is omitted again]. The strong copper-oxygen interactions cause a large bandwidth, steep bands, and consequently a broad DOS; these are the states that dominate near E_F. Furthermore, the Cu(1)-O(4) interactions lead to states with a strongly mixed DOS around 1 eV below E_F, and Cu(1) and O(1) mix between -5 and -7 eV. In the energy range where the copper DOS dominates and only a small admixture from oxygen states is found, we have essentially nonbonding Cu states which occur for Cu(1) near -2.5 eV and for Cu(2) around -2.5 and -1.5 eV.

The energy bands and site-projected DOS agree well with the recently published results of Oguchi, Sasaki, and Terakura[12] and Yu, Park, and Freeman.[13] Both of these papers present Fermi surfaces which are very similar to ours and thus are omitted here.

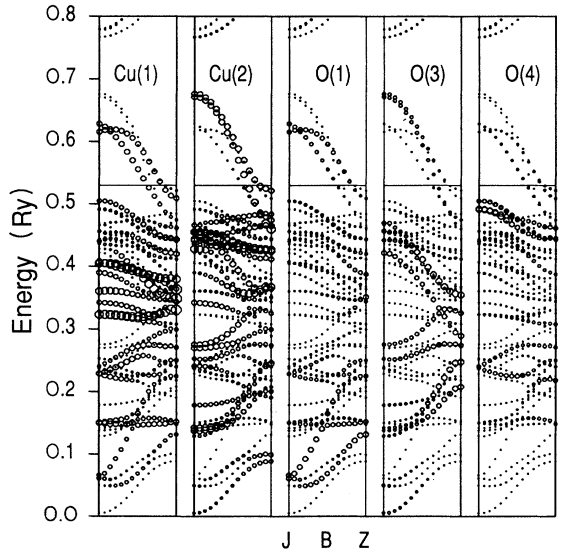

FIG. 4. Section of the band structure of Y-Ba-Cu-O_8 along the J-B-Z direction is shown 5 times, when the atomic weight of each band state is characterized by the size of the circle in the corresponding panel.

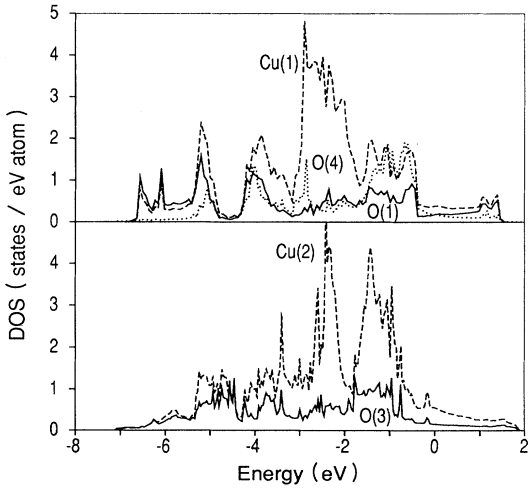

FIG. 5. Site-projected densities of states in states (including spin) per eV and atom (for notation see Fig. 1). The energy is with respect to E_F.

B. Charge distribution

In the LAPW formalism the symmetry decomposition of the electronic charge can be made according to *lm* inside the spheres, where the partial charges (Table I) correspond to the valence states of Y (5*s*, 5*p*, and 4*d*), Ba (6*s*, 5*p*, and 5*d*), Cu (4*s*, 4*p*, and 3*d*), and O (2*s*, 2*p*, and 3*d*). Note that often a large fraction of the charge (especially for transition metal *s* and *p* states) lies outside the atomic spheres and the partial charges depend on the choice of the sphere radii. In previous papers[9–11] we have demonstrated (especially for Cu and oxygen) that the partial charges reflect the interaction and are related to the nearest-neighbor distances. Short distances and strong (σ-type) interactions between Cu and O lead to broad-bands whose antibonding states are partly unoccupied, while weak interactions and longer distances cause narrow bands which are completely filled. In Y-Ba-Cu-O_7, for example, the chain O(1) has two Cu(1) neighbors at a short distance in the *b* direction, so that the strong interaction leads to a reduction of the oxygen p_y partial changes ($p_x=1.18$, $p_y=0.91$, and $p_z=1.25$ electrons).[11] In Y-Ba-Cu-O_8 the O(1) has a third Cu(1) neighbor in the *c* direction besides the two Cu(1) atoms in the *b* direction (Fig. 1). Therefore, the p_z charge of O(1) in Y-Ba-Cu-O_8 is smaller than that in Y-Ba-Cu-O_7 while the p_y charge remains the smallest and p_x becomes the largest component (Table I). The Cu(1) site of Y-Ba-Cu-O_8 has about 0.06 *d* electrons more in its sphere than in Y-Ba-Cu-O_7, while the planar oxygens O(2) and O(3) loose about 0.03 *p* electrons; the Cu(2) charge remains almost the same. These effects can be studied by electron difference densities, which will be discussed in the next section.

C. Electron densities

Figure 6 shows the charge distribution of Y-Ba-Cu-O_7 and Y-Ba-Cu-O_8 as difference electron densities $\Delta\rho$ in the (100) plane (see Fig. 1). $\Delta\rho$ is taken between the (LAPW) crystalline and the superposed ionic densities, which are constructed assuming the free ions Y^{3+}, Ba^{2+}, Cu^{+}, and oxygen with an ionicity of $-\frac{10}{7}$ in Y-Ba-Cu-O_7 and $-\frac{11}{8}$ in Y-Ba-Cu-O_8 (in order to keep electroneutrality in the ionic reference system). The negative contour lines correspond to a smaller charge in the crystal than in the superposed ions and indicate that the antibonding Cu-O orbitals are not fully occupied. The main difference between the two systems occurs at the O(1) position due to a strong coupling with the additional Cu(1) atom (threefold coordination in the double chain versus twofold in the linear chain). The large positive difference density at O(1) in the *c* direction, present in Y-Ba-Cu-O_7, disappears in Y-Ba-Cu-O_8, while its negative part in the *b* direction changes from -1.3 to $-0.9e/\text{Å}^3$, a value comparable to the other oxygen sites. Consequently, the principal component of the EFG is similar for all four oxygen positions (Table II; see Sec. IV D). The threefold coordination of O(1) leads to a buckling of the linar chain, the mirror plane is lost so that $\Delta\rho$ is asymmetric with respect to this plane. At the O(3) position the positive contour lines per-

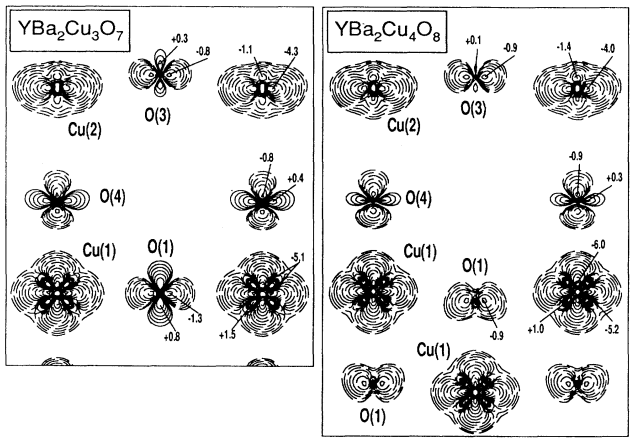

FIG. 6. Difference densities for Y-Ba-Cu-O_7 and Y-Ba-Cu-O_8 taken between the crystalline and the superposed ionic densities of Y^{3+}, Ba^{2+}, Cu^{+}, and $O^{-11/8}$ ($O^{-10/7}$) for Y-Ba-Cu-O_8 (Y-Ba-Cu-O_7). In both cases a contour plot is shown in a plane parallel to the *b* and *c* axes. Maxima and minima are labeled in units of $e/\text{Å}^3$; the lines start with ± 0.1 and differ by a factor of $\sqrt{2}$, where the solid (dashed) lines indicate positive (negative) values.

TABLE I. Partial charges (in electrons) of the valence states and their symmetry decomposition, where the cartesian coordinates are assumed to be parallel to the crystallographic axes: **x**||**a**, **y**||**b**, and **z**||**c**.

	s	*p*	*d*	*f*	p_x	p_y	p_z	d_{z^2}	$d_{x^2-y^2}$	d_{xy}	d_{xz}	d_{yz}
Y	0.177	0.262	0.882	0.133	0.086	0.085	0.091	0.088	0.233	0.079	0.244	0.238
Ba	0.059	5.565	0.286	0.073	1.862	1.857	1.866	0.059	0.037	0.097	0.051	0.042
Cu(1)	0.234	0.203	8.665	0.021	0.026	0.073	0.104	1.444	1.678	1.842	1.850	1.851
Cu(2)	0.204	0.184	8.696	0.017	0.076	0.073	0.035	1.749	1.456	1.851	1.819	1.821
O(1)	1.545	3.340	0.013	0.002	1.225	0.998	1.117	0.003	0.003	0.002	0.002	0.003
O(2)	1.532	3.363	0.011	0.001	1.000	1.196	1.167	0.002	0.003	0.003	0.002	0.001
O(3)	1.532	3.361	0.010	0.001	1.195	0.999	1.167	0.002	0.003	0.002	0.001	0.002
O(4)	1.537	3.364	0.009	0.001	1.177	1.193	0.994	0.004	0.000	0.001	0.002	0.002

TABLE II. Electric-field-gradient components (in 10^{21} V m^{-2}) for Y-Ba-Cu-O_8. The experimental data are taken from Zimmerman (Ref. 5).

Position		V_{aa}	V_{bb}	V_{cc}	V_{zz}	η
Cu(1)	theory	−5.1	6.1	−1.0	6.1	0.7
	experiment				±6.9	1.0
Cu(2)	theory	2.3	1.5	−3.8	−3.8	0.2
	experiment				∓11.6	0.0
O(1)	theory	−10.7	10.7	−0.0	10.7	1.0
O(2)	theory	11.2	−6.7	−4.5	11.2	0.2
O(3)	theory	−6.6	11.1	−4.5	11.1	0.2
O(4)	theory	−5.0	−6.5	11.5	11.5	0.1
Y	theory	−1.6	−1.6	3.2	3.2	0.0
Ba	theory	−6.1	−2.3	8.4	8.4	0.5

pendicular to the CuO_2 plane have almost disappeared in Y-Ba-Cu-O_8. This feature is independent of the small differences in the oxygen ionicities ($-\frac{10}{7}$ vs $-\frac{11}{8}$) of the reference system (superposed ionic densities) and is consistent with the smaller charge in O(3) with respect to Y-Ba-Cu-O_7 (Table II and Ref. 11).

D. Electric-field gradient

Table II summarizes the EFG tensor, the principal component V_{zz} (i.e., the largest of the three values), and the asymmetry parameter η. At present, experimental data are available only for the copper positions.[4,5] For the conversion from NQR frequencies to EFG's, we use the nuclear quadrupole moment $Q = -0.211b$ of ^{63}Cu by Sternheimer.[19] Good agreement between our theoretical and the experimental value is found for the Cu(1) position, while for Cu(2) the asymmetry of the EFG tensor agrees well, but the computed V_{zz} is much smaller than the experimental one,[4,5] so that the situation is very similar to Y-Ba-Cu-O_7.[9–11] We have shown previously that the EFG at the copper site originates from the asymmetric charge distribution of the $4p$ and $3d$ valence states. Furthermore, we have found that the p-p and d-d contributions to the EFG (especially for V_{20}) have opposite sign and cancel to a large extent (for definitions, see Ref. 11). At Cu(1) in Y-Ba-Cu-O_8, this cancellation leads to a small negative V_{20}, while V_{22} is large and again negative, so that [according to Eq. (1)] the components V_{aa} and V_{bb} are similar in magnitude; consequently, the asymmetry parameter η is close to unity and the EFG tensor points into the b direction. The EFG is dominated by the *valence* EFG (originating from the aspherical charge distribution inside the sphere), while the *lattice* EFG (the contribution from outside the sphere) is less than 2% for both copper positions. The effect of core polarizations is not very important, since the low-lying Cu $3p$ semicore states contribute, for example, less than 1% to the EFG of Cu(1).

In going from Y-Ba-Cu-O_7 to Y-Ba-Cu-O_7, one expects to see effects in the electronic structure for the chain oxygen O(1), since its coordination number is changed from two to three. It has been shown above (Secs. IV B and IV C) that a charge redistribution occurs, which affects the EFG as well. In Y-Ba-Cu-O_7 the O(1) site has copper neighbors only in the b direction leading to a large V_{bb} and a relatively small η of 0.3–0.4.[11] For Y-Ba-Cu-O_8, however, we predict for this position a reduced V_{bb} and an asymmetry parameter η of 1.0 (corresponding to a vanishing component in the c direction). The other oxygen positions are not much affected and thus have EFG's as in Y-Ba-Cu-O_7 and small η values. This change in the O(1) EFG makes all four oxygen EFG's comparable in magnitude, while in Y-Ba-Cu-O_7 the principal component at O(1) is about 50% larger than at the other oxygen sites and all four η values are small.

At the Y position the EFG is dominated by the semicore $4p$ states, which are high enough in energy to be affected by the surrounding ions, while the valence $5p$ (and $4d$) contributions are smaller. Although these results can not be checked experimentally, since none of the Y isotopes has a nuclear quadrupole moment, the Y EFG remains of interest from a theoretical point of view. The asymmetry parameter η has changed from 0.9 for Y-Ba-Cu-O_7 to 0.0 for Y-Ba-Cu-O_8, where in the latter case V_{aa} and V_{bb} are very similar. This is because the distances Y-O(2) and Y-O(3) are very similar in Y-Ba-Cu-O_8 (4.537 and 4.525 a.u.), but differ more in Y-Ba-Cu-O_7 (4.563 and 4.494 a.u.). Therefore, the xy anisotropy is small in Y-Ba-Cu-O_8, and consequently the semicore partial charges $4p_x$ and $4p_y$ agree to within 0.001 electrons, leading to an η of 0.

For Ba the EFG is dominated by the Ba $5p$ contribution and the main component V_{cc} is related to the smallest occupation number (p_z). The smallest EFG component V_{bb} is larger than in Y-Ba-Cu-O_7 and thus leads to a smaller η of 0.5 instead of 0.8 in Y-Ba-Cu-O_7. It is obvious that the EFG at the Ba site originates from the interactions with the oxygen neighbors, but since all four oxygens contribute to the EFG, no simple interpretation can be offered.

E. Core-level shifts

Recent measurements by x-ray photoelectron spectroscopy (XPS) have shown that the Ba core levels are shifted rigidly by about 0.4 eV to higher binding energies between Y-Ba-Cu-O_7 and Y-Ba-Cu-O_8.[20] It is well known

that the orbital energies of local-density-approximation (LDA) calculations should not be interpreted as excitation energies and thus do not correspond to ionization energies in contrast to Hartree-Fock calculations where this holds approximately according to Koopmans' theorem. However, the variation of the core binding energies (BE) between Y-Ba-Cu-O_7 and Y-Ba-Cu-O_8 can be estimated by taking the corresponding core energies with respect to E_F to yield the relative shifts. By using this simple approach, we find that all Ba core levels of Y-Ba-Cu-O_8 are about 0.35 eV lower in energy than those of Y-Ba-Cu-O_7, consistent with the higher binding energies observed experimentally. For Y we find that the core levels move up by about 0.15 eV, a shift so small that it was not detected in the recent experiment,[20] probably due to the limited resolution. The oxygen core-level shifts have not been studied experimentally.

We take the O 1s core energies with respect to E_F from the present calculation and the corresponding values from our previous work on Y-Ba-Cu-O_7 (Ref. 11) to predict the core-level shifts (Fig. 7). All values are with respect to a common reference, namely, the BE of O(4) in Y-Ba-Cu-O_7, which is the smallest BE, followed by O(1), O(3), and O(2), where the latter two are very similar. In Y-Ba-Cu-O_8 the O(1) level is drastically lowered in energy (i.e., changed to higher BE), an effect which is related to the higher stability of the chain oxygen. Since the O(1) charge is about the same in Y-Ba-Cu-O_7 and Y-Ba-Cu-O_8, this lowering comes mainly from the additional (third) Cu(1) ion surrounding O(1) with an increased Madelung stabilization. The O 1s levels of O(2) and O(3) move up and that of O(4) slightly down in energy, but the latter still has the smallest BE.

The oxygen core-level shifts have been studied by other recent LAPW calculations where our results differ from those by Yu, Park, and Freeman,[13] but are similar to the values quoted by Krakauer, Pickett, and Cohen[18] for Y-Ba-Cu-O_7. The discrepancy to the former values could come from computational differences such as the choice of different sphere radii for the inequivalent oxygen atoms which can affect the convergence.

In summary, the present calculations have shown that the electronic structure and charge distribution in Y-Ba-Cu-O_8 is quite similar to that of Y-Ba-Cu-O_7. The double copper-oxygen chain affects the electronic structure especially near the chain oxygen with a coordination of three copper neighbors. Here a significant change in the asymmetry of the charge distribution is found influencing the EFG, while the total charge at this O(1) site remains about the same. We find an increase of the Cu(1) charge by 0.06 d electrons and a related reduction of the O(2) and O(3) p charges. The charge transfer between the atoms shows the interplay between the chains and the plane and determines the number of holes in states near E_F.

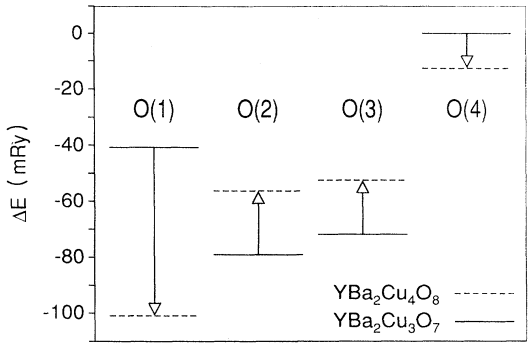

FIG. 7. Relative positions of the oxygen-core levels with respect to that of O(4) in Y-Ba-Cu-O_7 taken as reference. The Y-Ba-Cu-O_8 data are aligned in energy so that the two systems have a common Fermi energy.

ACKNOWLEDGMENTS

This project was supported by the "Fonds zur Förderung der wissenschaftlichen Forschung," project No. P7063P. Part of the extensive calculations were performed on the IBM 3090-400 VF of the computer center at the University of Vienna within the European Academic Supercomputing Initiative (EASI) sponsored by IBM; in part they were done on the Siemens VP-50 EX of the computer center at the Technical University of Vienna.

*Permanent address: Institut für Theoretische Physik, Universität Graz, A-8010 Graz, Universitätsplatz 5, Austria.

[1]J. Karpinski, E. Kaldis, E. Jilek, S. Rusiecki, and B. Buchner, Nature **366**, 660 (1988).

[2]E. Kaldis, P. Fischer, A. W. Hewat, E. A. Hewat, J. Karpinski, and S. Rusiecki, Physica C **159**, 668 (1989).

[3]B. Rupp, P. Fischer, E. Pöschke, R. R. Arons, and P. Meuffels, Physica C **156**, 559 (1988).

[4]H. Zimmermann, M. Mali, and D. Brinkmann, Physica C **159**, 681 (1989).

[5]H. Zimmermann, Ph.D. thesis, University of Zürich 1991 (and unpublished).

[6]P. Blaha, K. Schwarz, and P. Herzig, Phys. Rev. Lett. **54**, 1192 (1985).

[7]P. Blaha, K. Schwarz, and P. H. Dederichs, Phys. Rev. B **37**, 2792 (1988).

[8]P. Blaha and K. Schwarz, Hyperfine Interact. **52**, 153 (1989).

[9]C. Ambrosch-Draxl, P. Blaha, and K. Schwarz, J. Phys. Condens. Matter **1**, 4491 (1989).

[10]C. Ambrosch-Draxl, P. Blaha, and K. Schwarz, Physica C **162-164**, 1353 (1989).

[11]K. Schwarz, C. Ambrosch-Draxl, and P. Blaha, Phys. Rev. B **42**, 2051 (1990).

[12]T. Oguchi, T. Sasaki, and K. Terakura, Physica C **172**, 277 (1990).

[13]J. Yu, K. T. Park, and A. J. Freeman, Physica C **172**, 467 (1991).

[14]P. Blaha, K. Schwarz, P. Sorantin, and S. B. Trickey, Comput. Phys. Commun. **59**, 399 (1990).

[15]M. Weinert, J. Math. Phys. **22**, 2433 (1981).

[16]W. E. Pickett, Rev. Mod. Phys. **61**, 433 (1989).
[17]W. E. Pickett, R. E. Cohen, and H. Krakauer, Phys. Rev. B **42**, 8764 (1990).
[18]H. Krakauer, W. E. Pickett, and R. E. Cohen, J. Supercond. **1**, 111 (1988).
[19]R. M. Sternheimer, Z. Naturforsch. A **41**, 24 (1986).
[20]M. Shimoda, Y. Yamada, and T. Matsumoto, Physica C **171**, 444 (1990).